High Voltage

Special Issue: Selected Papers from the 2018 IEEE International Conference on High Voltage Engineering and Application (ICHVE 2018)

IET Journals
The Institution of Engineering and Technology

^{1}H NMR tests on damaged and undamaged XLPE and SiR samples

eISSN 2397-7264
Received on 28th March 2019
Revised 12th June 2019
Accepted on 4th July 2019
E-First on 19th August 2019
doi: 10.1049/hve.2019.0077
www.ietdl.org

Lydia Gkoura[1,2], Taiji Wang[3], Athanasios Anastasiou[1], Noureddine Harid[3] ✉, Huw Griffiths[3], Manu Haddad[4], Michalis Fardis[1], Marina Karayianni[1]

[1]*Institute of Nanoscience & Nanotechnology, National Centre for Scientific Research (NCSR), Demokritos, Athens, Greece*
[2]*School of Chemical Engineering, National Technical University of Athens, Athens, Greece*
[3]*Department of Electrical and Computer Engineering, Advanced Power and Energy Research Centre, Khalifa University, Abu Dhabi, United Arab Emirates*
[4]*School of Engineering, Advanced High Voltage Engineering Research Centre, Cardiff University, Cardiff, UK*
✉ *E-mail: noureddine.harid@ku.ac.ae*

Abstract: Cross-linked polyethylene (XLPE) and silicone rubber (SiR) samples were subjected to a high-voltage AC stress plane–plane configuration and inclined plane test, respectively. The voltage was applied such that discharge was observed across the surface of the XLPE test sample for several hours and for visible damage to occur on SiR samples also after several hours. Selected stressed samples together with virgin samples from the same manufactured batch were tested using nuclear magnetic resonance (NMR) spectroscopy. Specifically, ^{1}H NMR spin–lattice (T_1) and spin–spin (T_2) relaxation time measurements were employed to examine potential changes in the chemical bonding of undamaged and damaged XLPE and SiR samples. Preliminary results show that there may be a moderate increase in the T_1 and T_2 values of the damaged samples in comparison with the undamaged ones. This raises the possibility that NMR can be a useful additional experimental tool in characterising material degradation.

1 Introduction

Cross-linked polyethylene (XLPE) has become a dominant insulation material for cables in medium- and high-voltage systems due to its ability to operate at slightly higher temperatures and its ease and cheapness of production compared with traditional oil–paper technology. It is now considered that there may be limited further gains to be made in conventional XLPE material performance due to limits in achievable purity and operating temperature [1]. Nevertheless, the material continues to be extensively utilised, and its long-term performance is important to understand. In-service XLPE materials experience considerable electrical, thermal, and mechanical stresses under highly variable environmental conditions. Such conditions contribute to the deterioration of insulation performance and may lead ultimately to complete breakdown. Therefore, monitoring of XLPE insulation is important to the understanding of the ageing process, the reliability, and lifetime estimation of the insulation system as a critical component of the power system [2].

XLPE insulation under electrical stress in service may result in breaking of polymer chains and chemical bonds. For example, a break in a ∼C–H bond will release a hydrogen atom and a ∼C* polymeric free radical. There will be an increase in the number of H atoms, which can combine with other atoms to form hydrogen gas, whereas ∼C* polymeric free radicals may combine with other similarly formed radicals to stabilise themselves. Long-term partial discharge activity of XLPE cables under electrical and thermal stresses may lead to a discharge channel appearing in the form of electrical trees or water trees which conduct current across the voltage gap on insulators and metals leading to insulation failure. Many researchers have investigated this phenomenon and explored its temperature dependence [3–6].

Silicone rubber (SiR) insulation, on the other hand, has become extensively used in outdoor applications for high-voltage systems. The hydrophobic property of many polymeric materials that enable the transfer of hydrophobicity to an overlying pollution layer offers a significant advantage compared with glass or ceramic units used in overhead transmission and distribution systems in coastal or industrial environments. However, in spite of such inherent advantage, under severe ambient conditions, dry bands can still form, especially before hydrophobic recovery can occur in the pollution layer, and these are known to result in partial arc discharges in particular regions of insulator unit [7]. In particular, polymeric insulators are being used more extensively on overhead lines at voltages up to 132 kV, but concerns remain about their long-term performance in polluted atmospheric conditions. One of the main reasons that have contributed to this includes the effect of multi-ageing factors [8] that these insulators are subjected to under real service conditions such as electrical discharges, surface leakage current, and ultraviolet light, pollution.

Several techniques have been employed to assess the durability and structural integrity of polymers. Amongst commonly used techniques, we cite thermal analysis techniques such as differential scanning calorimetry [9], the X-ray diffraction technique to analyse the structural changes of thermally aged XLPE, spectroscopy techniques such as Fourier-transform infrared spectroscopy method, nuclear magnetic resonance (NMR) spectroscopy and dielectric spectroscopy [10–14], and mechanical strength testing techniques such as elongation at break and elasticity measurements [15]. Some researchers who used NMR techniques to investigate ageing and degradation have mainly focused on thermal ageing [15–20], and ageing due to partial discharge, electrical treeing, and water treeing [21–23]. Studies investigating erosion and tracking on SiR insulation and erosion due to surface discharge on XLPE insulation are very limited.

In this paper, the previous work reported by the authors on XLPE [24] is extended to study damage on both XLPE and SiR insulation samples using ^{1}H NMR measurements. The damage was artificially caused by accelerated electrical ageing leading to material erosion and tracking. In particular, the relaxation times of T_1 and ^{1}H nuclei within the molecules of the test sample material have been measured for undamaged and damaged samples.

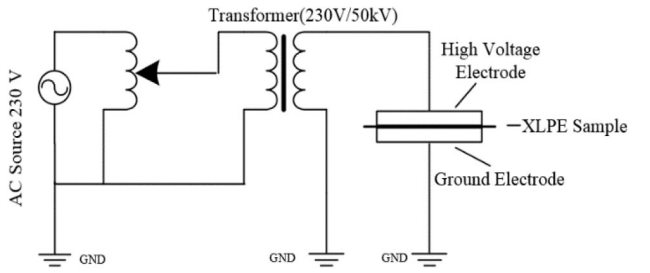

Fig. 1 *Schematic diagram of the setup for ageing of XLPE samples, operated at 12 kV, 50 Hz*

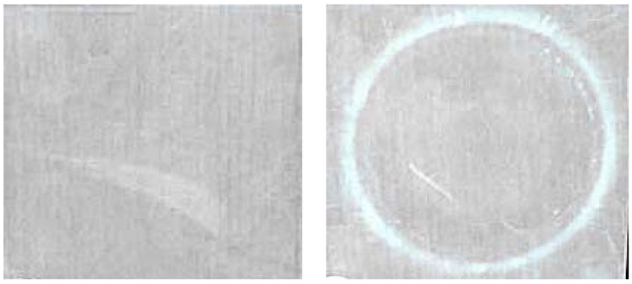

Fig. 2 *XLPE test samples*
(a) TR01528 undamaged sample, ***(b)*** TR01528 damaged sample

Experimental values of T_1 were acquired using the saturation recovery technique, whereas T_2 was measured by applying both the spin–echo pulse sequence and the Carr–Purcell–Meiboom–Gill (CPMG) pulse sequence with 20 and 30 μs duration between the π pulses, respectively.

2 Overview of NMR

NMR is one of the most valuable techniques able to provide detailed information on the local atomic arrangement and monitor atomic mobility and local interactions in real time. NMR spectroscopy is a versatile and non-invasive method; it can be applied on all three states of matter (liquid, solid, and gas), and under a wide range of conditions, in temperatures ranging from several mK to 1500 K, and pressures up to 4 kbars. In particular, solid-state NMR enables the investigation of polymers in both amorphous and semi-crystalline states with different shapes (e.g. powder, granules, and plate) without requiring special preparation procedures. The technique is based on the interaction of the nuclear spins with an external magnetic field, as well as on the interaction of nuclear spins with their neighbouring nuclear and unpaired electron spins [25]. This makes NMR extremely sensitive to the local atomic environment, enabling (i) the study of molecular and crystal structures at atomic-scale resolution and (ii) the study of atomic and molecular dynamics on multiple timescales ranging from nanoseconds to hours or even to weeks and months [26].

The dynamics of H containing molecules, in particular, are reflected in the spin–lattice and spin–spin relaxation processes occurring with characteristic relaxation times T_1 and T_2, respectively. The spin–lattice (or longitudinal) relaxation time describes the rate at which the equilibrium nuclear magnetisation along the static field is restored. This relaxation time is associated with dissipation processes from the spin system through all the other degrees of freedom (lattice), and thus, it allows obtaining information concerning the physical structure of the system. On the other hand, the spin–spin (or transverse) relaxation time T_2 describes the decay rate of the nuclear magnetisation components transverse to the applied static field, i.e. T_2 monitors the dephasing within the spin system, and therefore is able to provide information concerning dynamical processes such as spin diffusion [27].

NMR spectroscopy techniques have previously been applied to polymer materials for condition monitoring studies [17–20]. The effect of thermal ageing at different temperatures on the phase composition and molecular mobility of XLPE insulation samples extracted from high-voltage cable was studied by ^{1}H NMR relaxation time experiments [17]. The onset and progress of oxidation were observed to be very different for XLPE aged at different temperatures. In an earlier paper, the polymer–water interaction was investigated by detecting the ^{2}H and ^{13}C NMR by using the isotope substitution method [21]. It was found that the short and long components of T_2 indicated the existence of different environmental states in the water. Later, partial discharge and electrical treeing experiments were carried out on samples of low-density polyethylene [22, 23]. Proton NMR techniques were employed which focused on identifying morphological changes [25, 26], the results showed that only 10% natural deuterium determined by deuterium spectra and a short and long components of T_2 indicated the existence of different environmental states for the water. Research is expanding in the field of NMR applications with promising novel developments such as NMR sensors for on-site monitoring of outdoor insulation [28] and compact low-field NMR devices that offer the advantage of portability and on-site measurements [29].

3 Preparation of test samples

3.1 XPLE test sample preparation

3.1.1 Sample manufacture and ageing: XLPE samples were obtained from a leading plastic manufacturing company. All the samples were obtained from the same production run to guarantee that they would initially possess very similar physical and chemical properties, providing an objective reference base for subsequent testing. Fig. 1 shows the schematic diagram of the experimental platform used for the ageing of the XLPE test samples consisting of a 230 V AC source, a 230 V/50 kV HV transformer, and the plane–plane test cell containing the XLPE test sample. The dimensions of the XPLE test samples are $90 \times 90 \times 1$ mm^3. The test cell electrodes consist of circular steel sections, having a 75 mm diameter and 25 mm thickness.

The XLPE samples were aged by applying a continuous 12 kV, 50 Hz AC test voltage across the test sample in a plane–plane electrode configuration for 10 h. This voltage is ∼90% of the partial discharge extinction voltage, contributing to damaging and ageing of the XLPE samples. Fig. 2*a* shows a virgin sample, whereas Fig. 2*b* shows a damaged XLPE sample identified by a visible eroded area immediately around the periphery of the HV electrode.

3.1.2 NMR test batch preparation: In NMR tests, the quality of samples has a significant influence on the NMR spectrum, and careful sample preparation is essential. Accordingly, solid particles sticking to the sample surface were removed; otherwise, these may distort magnetic field homogeneity and lead to an incorrect spectrum. In this experiment, the damaged and undamaged samples were cut into strips having dimensions of $1 \times 1 \times 30$ mm^3, and the strips were formed into cylindrically bundled test specimens, as shown in Fig. 3. It is evident that the damaged samples are significantly discoloured compared with the undamaged samples, which may have resulted from chemical property changes under the long-term high-voltage stress. The test bundle samples were placed into the NMR test tube to a specific depth to avoid distortion of the field homogeneity caused by the ends of each sample.

3.2 SiR test sample preparation

3.2.1 Sample manufacture and ageing: Test specimens were moulded from liquid SiR provided by a leading manufacturer. The specimens were cured at room temperature for a minimum 24 h, followed by 3 h post-curing at 120°C. The mould was designed to produce rectangular specimens of dimensions 120 mm × 50 mm and thickness 6 mm with two plane surfaces.

Selected test specimens were subjected to an accelerated ageing process in the laboratory with the liquid contaminant and an inclined arrangement of the samples as specified in IEC 60587. As shown in Fig. 4, with an incline of 45°, a test voltage of 3.5 kV

a *b*

Fig. 3 *NMR test samples*
(a) TR01528 undamaged sample, ***(b)*** TR01528 damaged sample

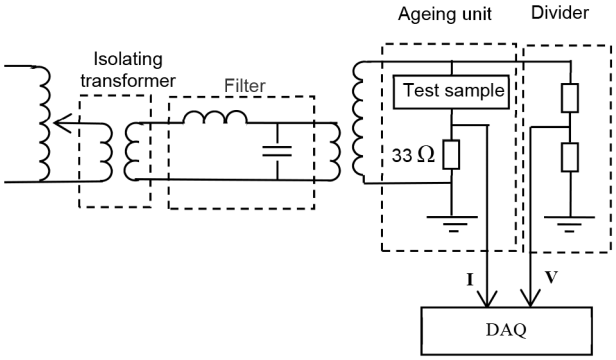

Fig. 4 *Schematic diagram of the setup for ageing of SiR*

root mean square was applied across the test electrodes at a separation of 50 mm for 6 h. Ammonium chloride solution with a concentration 0.1% was used as the contaminant with a flow rate of 0.30 ml/min. Since the tests are designed to promote arcing, the specimens in these tests were highly stressed electrically. One of the aged samples is shown in Fig. 5, where significant erosion can be seen in the central region.

3.2.2 NMR test batch preparation: The aged SiR specimen was cut into small sub-samples of suitable volumes for NMR testing. Concerning Fig. 5 schematic view, sub-sample 'S1' was taken from the damaged central region of DC1DU, whereas sub-sample 'S2' was taken from the undamaged region on the left-hand side of DC1CU.

4 ^{1}H NMR relaxation time measurement

4.1 XLPE samples

4.1.1 ^{1}H NMR measurements of T_1: All NMR measurements were taken in the fringe field of a 4.7 T Bruker superconducting magnet shown in Fig. 6. The magnet provides a 34.7 T/m constant field gradient and a perturbation with a given ^{1}H NMR frequency. For all measurements, the position of the sample in the magnetic field was the same, corresponding to a ^{1}H NMR frequency of 101.989 MHz, as shown in Fig. 6. T_1 was measured using a standard saturation recovery technique, and the signal was detected by the common Hahn–echo pulse sequence.

The saturation recovery technique is commonly used to measure T_1 and is very effective to obtain accurate line shapes, especially if the shape of the signal is very broad or not easily inverted [12]. The Hahn–echo pulse sequence, also called the spin–echo pulse sequence, is the most common sequence applied in

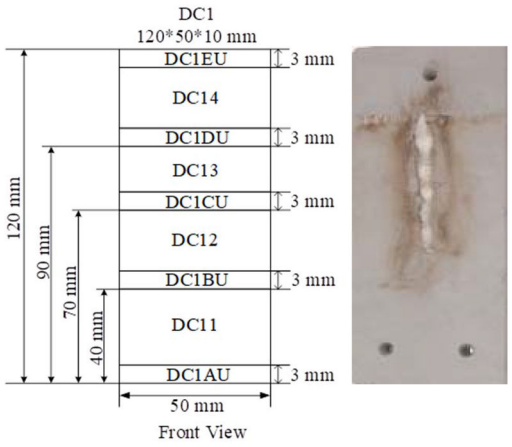

Fig. 5 *Aged SiR test sample*

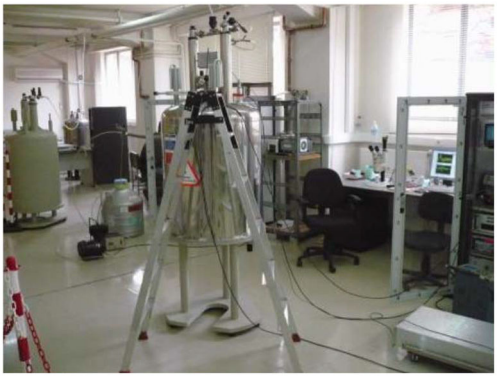

Fig. 6 *4.7 T Bruker superconducting magnet with 34.7 T/m constant field gradient at NCSR, Demokritos*

NMR experiments based on refocusing of spin magnetisation by a pulse of resonant electromagnetic radiation [13]. The 90° radio-frequency pulses are employed to excite the magnetisation and one or multiple 180° pulses to generate signal echoes by refocusing the spins. The ^{1}H NMR relaxation time experiments were performed with the pulse sequence $\pi/2$–VD–$\pi/2$–τ–π–τ–signal, where VD is the variable delay time for magnetisation recovery. The $\pi/2$ pulse was 5 μs.

Since the different numbers of scans were used in each measurement, different signal amplitudes between damaged and undamaged samples were obtained. Hence, to represent the general trend of the relaxation amplitude more accurately, we used the relative 'concentration' of each component rather than the absolute amplitude. The relative concentration is defined by the ratio S/S_0, where S denotes the echo amplitude acquired during the ^{1}H T_1 measurements and S_0 is the signal amplitude corresponding to the equilibrium magnetisation value.

Fig. 7 depicts plots of the ratio S/S_0 as a function of the VD for damaged and undamaged samples. In this figure, the experimental magnetisation recovery curves could be fitted by a one-phase exponential function of the form

$$S = S_0 \cdot \left(1 - A\mathrm{e}^{-(x/T_1)}\right) \tag{1}$$

The ^{1}H T_1 values resulting from the corresponding fits are 313 ms for the undamaged samples and 334 ms for the damaged samples.

4.1.2 ^{1}H NMR measurements of T_2: T_2 measurements of undamaged and damaged samples were conducted using the common Hahn–spin–echo pulse sequence: $\pi/2$–VD–π–VD–signal. Fig. 8 illustrates the fit of the experimental transverse magnetisation decay curves with single- and double-exponential decay functions. As can be readily observed, the Hahn–spin–echo decay curves cannot be accurately represented by a single-

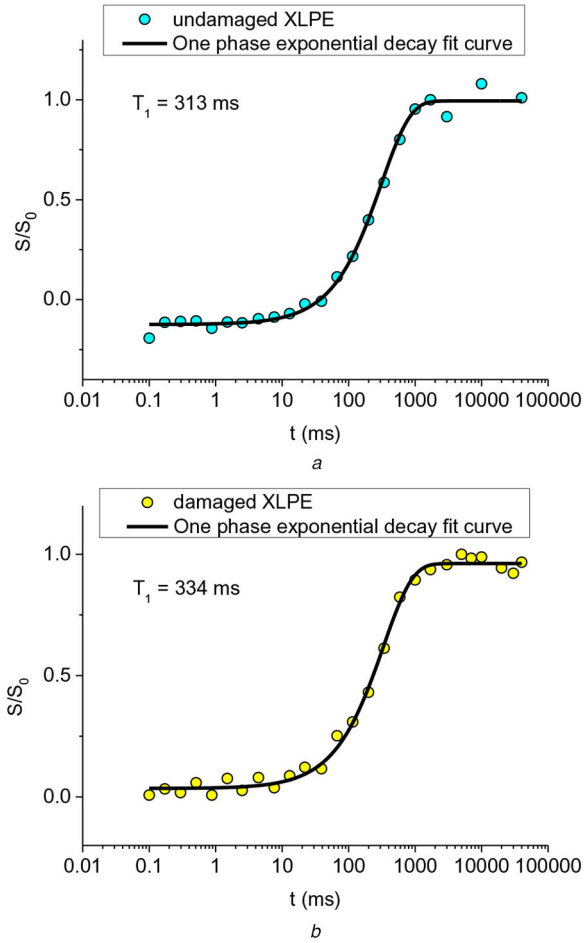

Fig. 7 *^1H NMR T_1 measurements by the saturation recovery spin–echo pulse sequence*
(a) Undamaged sample, ***(b)*** Damaged sample

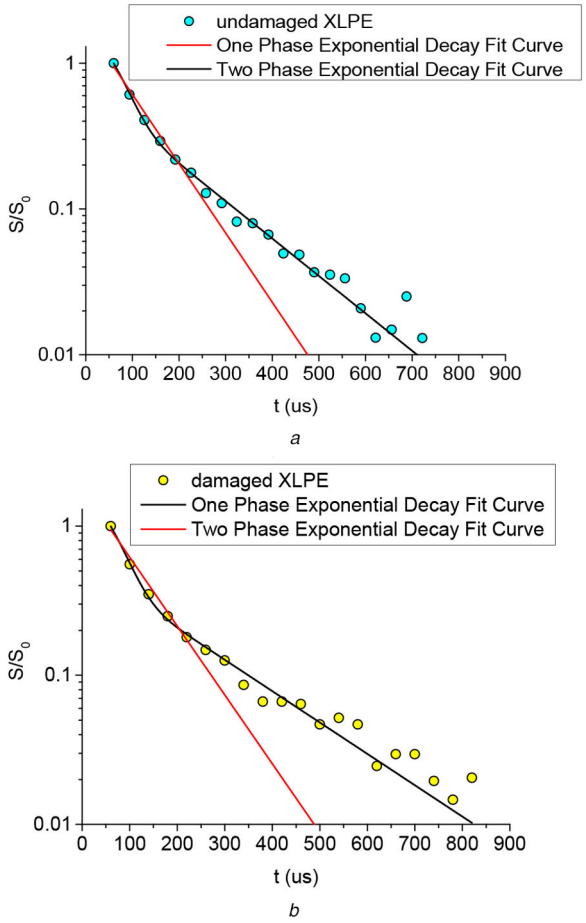

Fig. 8 *^1H NMR T_2 measurements by Hahn–spin–echo pulse sequence*
(a) Undamaged sample, ***(b)*** Damaged sample. For comparison, a mono-exponential fitting is shown with a red line

exponential function. Instead, two T_2 components may be identified: a rapidly decaying signal that could be fitted with a Gaussian function and a much more slowly decaying component that has been approximated by an exponential decay. Similar behaviour has also been reported for the ^{1}H transverse relaxation in polyolefin resins [30], where a double-exponential function is of the form

$$S = S_{01}e^{-(x/T_{21})^2} + S_{02}e^{-(x/T_{22})} \quad (2)$$

has been used to fit the corresponding decay curves. The resulting values of the two T_2 components for both damaged and undamaged samples are given in Table 1 together with the relative per cent concentrations A_1 and A_2 of the two phases corresponding to the short and long T_2 components, respectively, and given by

$$A_1 = \frac{S_{01}}{S_{01} + S_{02}}, \quad (3a)$$

$$A_2 = \frac{S_{02}}{S_{01} + S_{02}} \quad (3b)$$

By inspecting Table 1, it is deduced that in both cases the dominant contribution to the transverse relaxation stems from the fast relaxing component which is associated with the rigid regions (rigid phase) of the polymer.

4.1.3 ^1H NMR T_2 measurements with the CPMG pulse sequence: T_2 measurements were also performed by applying a CPMG pulse sequence with more than 100 pulses. The CPMG spin–echo sequence $\pi/2-\{\tau-\pi-\tau\}_n$ comprises a 90° pulse that creates the transverse magnetisation and a train of n repetitive 180 pulses separated by equal time intervals 2τ and generating successive spin–echoes in the mid-time interval between each pair of consecutive π pulses. Two different CPMG experiments were conducted for both samples with 20 and 30 μs durations between the π pulses. The experimental curves are presented in Fig. 9 and were fitted with the same double-exponential function as the Hahn–spin–echo decays. To facilitate comparison between measurements obtained with the 20 and 30 μs time intervals, the normalised values of the magnetisation are used. However, since the repeated application of successive 180 pulses serves to supress inhomogeneities, longer relaxation times are, in general, anticipated with the CPMG pulse sequence as compared with the T_2 values found with the Hahn–spin–echo decay technique. The values and relative per cent concentrations of the two T_2 components resulting from the fitting of the transverse magnetisation decays observed with the CPMG pulse sequence are given in Table 2.

Table 1 ^{1}H NMR T_2 measurements by Hahn–echo pulse sequence

Hahn–spin–echo	T_{21} first component		T_{22} second component	
	A_1, %	T_{21}, μs	A_2, %	T_{22}, μs
undamaged	58	81	42	169
damaged	65	83	35	206

4.2 SiR samples

4.2.1 ^1H NMR T_1 measurements: For the SiR samples, ^{1}H NMR T_1 measurements were carried out using the 4.7 T Bruker superconducting magnet with a ^{1}H NMR frequency of 200.787

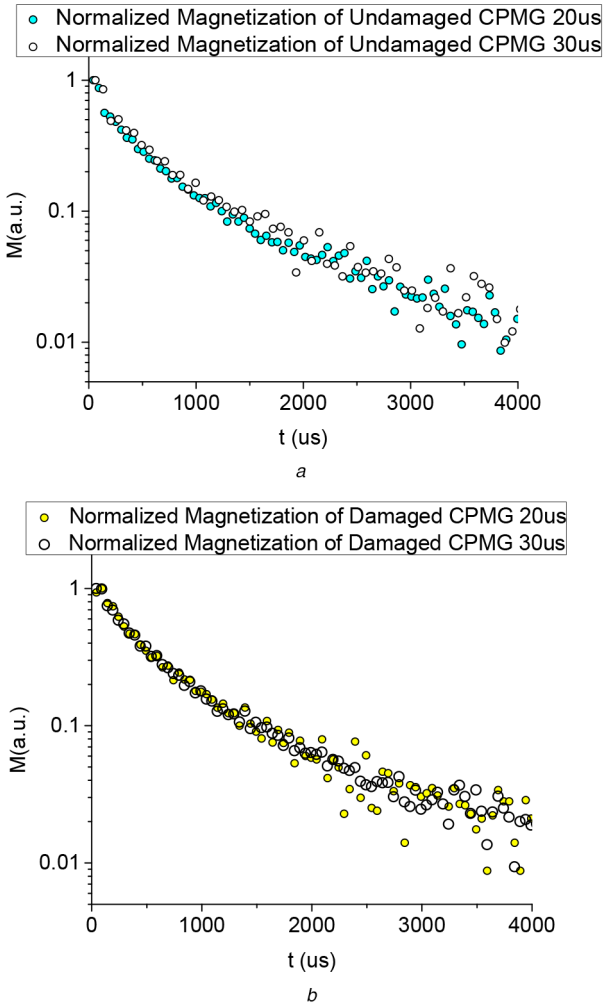

Fig. 9 *^1H NMR T_2 measurements by the CPMG spin–echo pulse sequence*
(a) TR01528 undamaged sample, ***(b)*** TR01528 damaged sample

Table 2 ^{1}H NMR T_2 measurements with the CPMG spin–echo pulse sequence: XLPE sample

	T_{21} first component		T_{22} second component	
CPMG 20 μs	A_1, %	T_{21}, μs	A_2, %	T_{22}, μs
undamaged	53	130	47	780
damaged	52	260	48	987
CPMG 30 μs	A_1	T_{21}, μs	A_2	T_{22}, μs
undamaged	53	136	47	918
damaged	52	250	48	940

MHz at the centre of the magnetic field. As with the XLPE sample tests, T_1 was measured using a standard saturation recovery technique, and the signal was detected by the common Hahn–echo pulse sequence. The same pulse sequence $\pi/2$–VD–$\pi/2$–τ–π–τ–signal was applied with the $\pi/2$ pulse set to 30 μs.

Fig. 10 shows the ^{1}H T_1 measurement on damaged and undamaged samples. A similar analysis as for the XLPE samples was applied to the experimental curves yielding T_1 values of 1.03 and 1.02 s for the undamaged samples and damaged samples, respectively. As we can observe, there is no significant difference between the T_1 values for the undamaged samples and the damaged ones.

4.2.2 ^1H NMR T_2 measurements: T_2 measurements of undamaged and damaged samples were conducted using the same Hahn–spin–echo pulse sequence as the one adopted for the XLPE samples, and the results are shown in Fig. 11. By comparing the corresponding spin–echo decays observed in the XLPE (Fig. 8) and

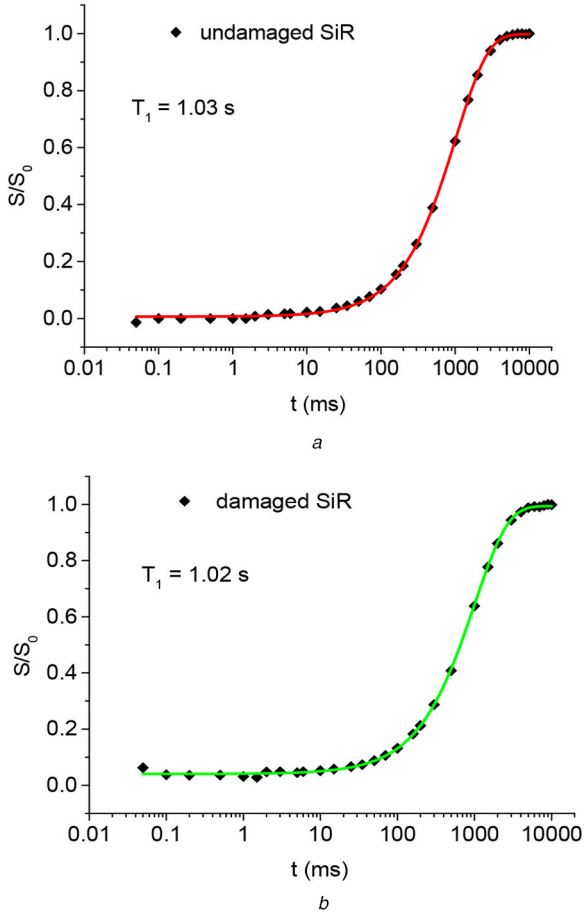

Fig. 10 *^1H NMR T_1 measurements by the spin–echo pulse sequence*
(a) Undamaged sample, ***(b)*** Damaged sample

SiR (Fig. 11) samples, it is easily deduced that the transverse magnetisation decay is much slower in SiR, probably corresponding to more flexible structures, and therefore characterised by longer relaxation times. Indeed, in the case of SiR, the experimental data could be fitted by a double-exponential function comprising of two Lorentzian exponential contributions of the form

$$S = S_{01}e^{-(x/T_{21})} + S_{02}e^{-(x/T_{22})} \quad (4)$$

The values of the two T_2 components and their relative per cent concentrations resulting from the fitting procedure are presented in Table 3. As can be seen, the fast relaxing component dominates almost completely the transverse magnetisation relaxation in the undamaged SiR sample, with only a minor contribution from the slowly relaxing component, indicating a predominance of the rigid over the amorphous regions in the pristine SiR. However, after the application of electrical stress, both T_2 values are enhanced, while simultaneously a small increase in the percentage of the long T_2 component is found. This might indicate an increase of the less rigid amorphous regions of the sample resulting possibly from the breaking of cross-linking bonds and/or chemical bonds on electrical stress treatment.

5 Conclusions

Preliminary ^{1}H NMR tests were carried out on undamaged and damaged XLPE and SiR samples by measuring the relaxation times T_1 and T_2. The results of these tests show that NMR relaxation measurements may be used as a qualitative or quantitative tool to evaluate ageing of XLPE and SiR. During the laboratory ageing process, the specimens were subjected to high electrical stress resulting in a diverse variety of possible chemical structure changes such as the shortening of the polymer or silicone chains and the

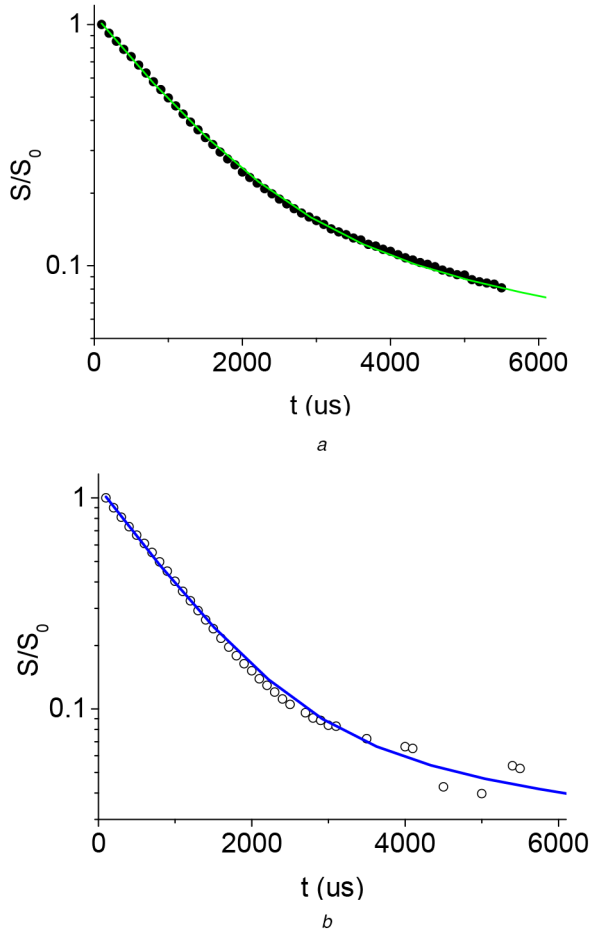

Fig. 11 *^{1}H NMR T_2 measurements by Hahn–spin–echo pulse sequence*
(a) Undamaged sample, ***(b)*** Damaged sample

Table 3 ^{1}H NMR T_2 measurements by Hahn–echo pulse sequence: SiR sample

	T_{21} first component		T_{22} second component	
Hahn–spin–echo	A_1, %	T_{21}, μs	A_2, %	T_{22}, μs
undamaged	93	850	7	8600

breaking of the chemical ∼C–H bonds and of the cross-linking bonds. These mechanisms alter the relative concentrations of rigid and amorphous phases present in the solid polymers, and can in principle be detected by the ^{1}H NMR relaxation measurements. Indeed, ^{1}H T_2 measurements in XLPE and SiR samples, both prior and after electrical stress treatment, revealed the presence of two components in the decay of the transverse magnetisation: a fast decay component and a more slowly relaxing one corresponding to ^{1}H in the 'rigid' and in the amorphous regions of the polymers, respectively. Modifications in the chemical structure of the damaged polymers are thus reflected in the observed values and the relative concentrations of the fast and slow T_2 components. Overall, it was found that:

- A single spin–lattice ^{1}H relaxation time T_1 was observed in both XLPE and SiR samples in contrast to the two components found for T_2. This behaviour is commonly encountered in solid polymers [28–30] and can be explained in terms of spin diffusion, resulting in energy transfer among ^{1}H spins on a time scale faster than spin–lattice relaxation processes, but slower compared with the T_2 processes. Moreover, no significant change was observed in the T_1 values due to electrical stress damage, except for a slight increase in the case of XLPE, and this fact could also be attributed to the effect of fast spin diffusion.
- Regarding ^{1}H T_2 measurements in the XLPE samples, two T_2 components were identified, a fast decaying Gaussian component assigned to protons in the rigid regions of the sample and a slower Lorentzian component stemming from the relaxation of protons in the amorphous regions of the polymer. Both components were found to increase on the application of high electrical stress, probably indicating an increase of the amorphous 'phase' as a result of cross-linking bonds breaking in the damaged samples. In the XLPE samples, both Hahn–spin–echo and CPMG pulse sequences techniques were applied for the T_2 measurements, and were shown to exhibit the same trend with the observed decays resulting from either pulse sequence comprising of a fast and a slow relaxing component, while the resulting T_2 values from both methods were found to increase after electrical stress treatment possibly reflecting bond breaking leading to enhanced flexibility.
- In the SiR samples, T_2 measurements were performed with the Hahn–spin–echo pulse sequence, showing similar results regarding the enhancement of flexible amorphous regions on application of high electrical stress. Since the application of the CPMG and the Hahn pulse sequences in the case of XLPE samples gave similar information regarding the decay of the transverse magnetisation and the 'amount' of rigid and amorphous phases in the polymers, it was deemed that no further information could be obtained by applying the CPMG measurements in the SiR samples.

Further validating tests on both XLPE and SiR samples are required, and it is proposed that these include NMR tests on samples with varying degrees of discharge-induced damage.

6 Acknowledgments

The authors are grateful for the support provided by the APEC Centre, Khalifa University, the National Centre for Scientific Research 'Demokritos' in Greece, where the NMR tests were carried out, and the Cardiff University for providing the SiR test samples.

7 References

[1] Andritsch, T., Vaughan, A., Stevens, G.C.: 'Novel insulation materials for high voltage cable systems', *IEEE. Electr. Insul. Mag.*, 2017, **33**, (4), pp. 27–33
[2] Bessissa, L., Boukezzi, L., Mahi, D., *et al.*: 'Lifetime estimation and diagnosis of XLPE used in HV insulation cables under thermal ageing: arithmetic sequences optimized by genetic algorithms approach', *IET Gener. Trans. Distrib.*, 2017, **11**, (10), pp. 2429–2437
[3] Wenbiao, T., Shuyong, S., Wei, Z., *et al.*: 'Influence of temperature on the growth characteristics of water tree in XLPE cable', *J. Eng.*, 2019, **2019**, (16), pp. 1636–1639
[4] Liu, Y., Cao, X., Chen, G.: 'Electrical tree initiation in XLPE cable insulation under constant DC, grounded DC, and at elevated temperature', *IEEE Trans. Dielectr. Electr. Insul.*, 2018, **25**, (6), pp. 2287–2295
[5] Li, L., Zhong, L., Zhang, K., *et al.*: 'Temperature dependence of mechanical, electrical properties and crystal structure of polyethylene blends for cable insulation', *Materials*, 2018, **11**, pp. 1–9, Art. No. 1922
[6] Su, Y., Liu, Y., Zhong, L.: 'Evaluation of voltage endurance characteristics for new and aged XLPE cable insulation by electrical treeing test', *IEEE Trans. Dielectr. Electr. Insul.*, 2019, **26**, (1), pp. 72–80
[7] Waters, R.T., Haddad, A., Griffiths, H., *et al.*: 'Dry-band discharges on polluted silicone rubber insulation: control and characterization', *IEEE Trans. Dielectr. Electr. Insul.*, 2011, **18**, (6), pp. 1995–2003
[8] Spellman, C., Young, H.M., Haddad, A., *et al.*: 'Survey of polymeric insulator ageing factors'. Proc. 11th Int. Symp. High Voltage Engineering (ISH), London, UK, 1999, vol. **4**, pp. 160–164
[9] Boukezzi, L., Boubakeur, A., Laurent, C., *et al.*: 'DSC study of artificial thermal aging of XLPE insulation cables'. Int. Conf. Solid Dielectrics, Winchester, UK, 2007, pp. 146–149
[10] Gulmine, J.V., Akcelrud, L.: 'FTIR characterization of aged XLPE', *Polym. Test.*, 2006, **25**, pp. 932–942
[11] Labouriau, A., Cox, J.D., Schoonover, J.R., *et al.*: 'Mossbauer, NMR and ATR-FTIR spectroscopic investigation of degradation in RTV siloxane foam', *Polym. Degradation Stab.*, 2006, **92**, (3), pp. 285–292
[12] Ohki, Y., Hirai, N., Min, D., *et al.*: 'Degradation of silicone rubber analyzed by instrumental analyses and dielectric spectroscopy'. Proc. 18th Int. Conf. Environmental Degradation of Materials in Nuclear Power Systems – Water Reactors. The Minerals, Metals & Materials Series, 2019, pp. 1323–1332
[13] Andjelkovic, D., Rajakovic, N.: 'Influence of accelerated aging on mechanical and structural properties of cross-linked polyethylene (XLPE) insulation', *Electr. Eng. (Arch. Elektrotech.)*, 2001, **83**, (1–2), pp. 83–87

[14] Linde, E., Verardi, L., Pourmand, P., *et al.*: 'Non-destructive condition monitoring of aged ethylene–propylene copolymer cable insulation samples using dielectric spectroscopy and NMR spectroscopy', *Polym. Test.*, 2015, **46**, pp. 72–78

[15] Zhang, J., Adams, A.: 'Understanding thermal aging of non-stabilized and stabilized polyamide 12 using ^{1}H solid-state NMR', *Polym. Degradation Stab.*, 2016, **134**, pp. 169–178

[16] Teymouri, Y., Kwamen, R., Blümich, B.: 'Aging and degradation of LDPE by compact NMR', *Macromol. Mater. Eng.*, 2015, **300**, pp. 1063–1070

[17] Paul, J., Hansen, E.W., Jaan Roots, J.: 'Probing the molecular dynamics in XLPE aged at different temperatures by ^{1}H NMR relaxation time measurements', *Polym. Degradation Stab.*, 2012, **97**, pp. 2403–2411

[18] Budrugeac, P., Segal, E.: 'Changes in the mechanical properties and thermal behaviour of LDPE in response to accelerated thermal aging', *J. Therm. Anal. Calorimetry*, 1998, **53**, pp. 801–808

[19] Boukezzi, L., Boubakeur, A., Lallouani, M.: 'Effect of artificial thermal aging on the crystallinity of XLPE insulation cables: X-ray study'. Int. Conf. Electrical Insulation and Dielectric Phenomena Annual Report, 2007, pp. 65–68

[20] Numata, K., Kurokawa, H., Sekine, S., *et al.*: 'Determination of limiting values of ^{1}H spin–spin relaxation time to assess lifetime of thermally aged acrylonitrile butadiene rubber', *Polym. Degradation Stab.*, 2019, **162**, pp. 12–21

[21] Abdolall, K.: 'The polymer–water interaction in water treeing: an NMR study'. Conf. Record of the 1988 IEEE Int. Symp. Electrical Insulation, Cambridge, MA, 1988, pp. 267–271

[22] Weigand, F., Spiess, H.W., Blumich, B., *et al.*: 'Nuclear magnetic resonance imaging of electrical trees in PE', *IEEE Trans. Dielectr. Electr. Insul.*, 1997, **4**, (3), pp. 280–285

[23] Blumler, P., Paus, N., Salge, G.: 'Nuclear magnetic resonance imaging of morphological changes during electrical treeing in polyethylene due to partial discharges'. Proc. 1998 IEEE Sixth Int. Conf. Conduction and Breakdown in Solid Dielectrics ICSD '98, Vasteras, Sweden, 1988, pp. 168–172

[24] Wang, T., Gkoura, L., Harid, N., *et al.*: '^{1}H NMR tests on damaged and undamaged XLPE samples'. IEEE Int. Conf. High Voltage Engineering and Application, Athens, Greece, 2018, pp. 1–4, paper 1435-550219

[25] Macomber, R.S.: '*A complete introduction to modern NMR spectroscopy*' (John Wiley & Sons, Inc., New York, NY, USA, 1998)

[26] Bruch, M.D.: '*NMR spectroscopy techniques*' (Marcel Dekker, New York, NY, USA, 1996)

[27] Fukushima, E., Roeder, S.B.W.: '*Experimental pulse NMR: a nuts and bolts approach*' (Addison-Wesley Publishing Company, Reading, MA, USA, 1981)

[28] Zheng, X., Xianjun, C., Kaikai, M., *et al.*: 'Novel unilateral NMR sensor for assessing the aging status of silicone rubber insulator', *IEEE Sens. J.*, 2016, **16**, (5), pp. 1168–1175

[29] Adams, A.: 'Non-destructive analysis of polymers and polymer-based materials by compact NMR', *Magn. Res. Imag.*, 2019, **56**, pp. 119–125

[30] Doolan, K.R.: 'Nuclear magnetic relaxation in polyolefin resins', *J. Polym. Sci. B, Polym. Phys.*, 2002, **40**, pp. 572–584